Diagnostic Performance of Advanced MRI in Differentiating High-Grade from Low-Grade Gliomas in a Setting of Routine Service

Orasa Chawalparit MD*, Tumtip Sangruchi MD**, Theerapol Witthiwej MD***, Sith Sathornsumetee MD****, Sirion Tritrakarn MD*, Siriwan Piyapittayanan MD*, Prapaluck Chaicharoen MD*, Thanyaporn Direksunthorn MD*, Panida Charnchaowanish BSc*

** Departments of Radiology, Faculty of Medicine Siriraj Hospital, Mahidol University, Bangkok, Thailand*
*** Departments of Pathology, Faculty of Medicine Siriraj Hospital, Mahidol University, Bangkok, Thailand*
**** Departments of Surgery, Faculty of Medicine Siriraj Hospital, Mahidol University, Bangkok, Thailand*
***** Departments of Medicine, Faculty of Medicine Siriraj Hospital, Mahidol University, Bangkok, Thailand*

Objective: *To evaluate the usefulness of advanced MRI techniques in differentiating high-grade (HGG) from low-grade gliomas (LGG).*
Material and Method: *Sixty-four patients with suspected gliomas were prospectively evaluated by conventional and advanced MRI studies including MR spectroscopy (MRS), diffusion tensor imagining (DTI), and dynamic susceptibility contrast (DSC) MRI. The parametric measurements of metabolic profile, cerebral blood volume, flow (CBV, CBF), apparent diffusion coefficient (ADC), fractional anisotropy, and their ratios by internal normalization were analyzed to differentiate LGG from HGG. Histopathologic findings were used as the gold standard.*
Results: *Forty-three cases with pathologically-proven gliomas were included. The best discriminating features between HGG and LGG were CBV and CBF of the solid tumoral region ($p<0.05$) whereas the minADC/corpus callosum ratio for DTI and the ratio of Cho/Cr for MRS of the solid tumoral region provided the best diagnostic performance ($p<0.05$). With a predetermined threshold for each parametric measurement, the combination of all advanced MRI modalities was associated with the best accuracy whereas the combination of DSC MRI and MRS provided the highest specificity. When all parametric measurements were positive, the probability of HGG was 0.889.*
Conclusion: *Comprehensive advanced MRI studies provided better diagnostic performance than using conventional MRI alone in the evaluation of gliomas.*

Keywords: *Gliomas, MRI, Advanced*

J Med Assoc Thai 2013; 96 (10): 1365-73
Full text. e-Journal: *http://jmat.mat.or.th*

Gliomas are the most common primary intra-axial neoplasm of the brain. The mean survival rate of glioblastoma (GBM), the most common primary brain tumor in adults, remains poor with a two-year survival rate less of than 10%[1]. Therapeutic strategies, treatment response, and prognosis for gliomas differ considerably depending on the tumor histologic grade. Therefore, identification of the highest grade portion by surgical biopsy or resection is an important and challenging issue. Furthermore, because of the tumor heterogeneity, an inaccurate biopsy site or inadequate sample may lead to an erroneous interpretation of the tumor grade and subsequently an inappropriate treatment regimen[2]. Glioma cells are known to infiltrate the brain parenchyma by following the vascular routes or tracking along the white matters[3]. The uncontrollable proliferation of the tumor cells contributes to hypercellularity of the lesion. An increasing metabolic demand induces angiogenesis or formation of new blood vessels[4]. Tumor blood vessels are histologically abnormal with more permeability than normal vessels. These vascular abnormalities and altered flow dynamics lead to changes in blood volume and flow[5].

Conventional MRI (cMRI) is not adequate to characterize histologic type and grade of tumors. Kondziolka et al demonstrated a 50% false-positive rate in determining supratentorial gliomas[6]. Another study reported almost one-fifth of GBMs did not

Correspondence to:
Chawalparit O, Department of Radiology, Faculty of Medicine Siriraj Hospital, 2 Prannok Road, Bangkok 10700, Thailand.
Phone: 0-2419-7086, Fax: 0-2412-7785
E-mail: oak_art@yahoo.com

show enhancement after intravenous contrast administration[7].

Novel MRI techniques are promising for tissue characterization in histologic and metabolic profiles. Many previous studies reported superiority of the advanced MRI (aMRI) such as MR spectroscopy (MRS), perfusion MRI (pMRI) and diffusion tensor imaging (DTI) to cMRI in differentiating high grade (HGG) from low grade gliomas (LGG)[8,9]. Due to the complexity and time-consuming nature in performing an aMRI, performing these pulse sequences in resource-poor setting presents a challenge. In order to increase the utilization of these aMRI techniques, which are commercially available in most new generation MR machines, a precise protocol is required, with a prospectively identified diagnostic performance evaluation of each aMRI modality. In this study, the authors attempt to elucidate diagnostic performance of MRS, DTI and pMRI to differentiate HGG from LGG. The results from the present study are expected to serve as a guideline for interpretation of aMRI at our institution and encourage clinicians to use advanced study techniques as a routine imaging procedure for the management of patients with suspected gliomas.

Material and Method

Patients

Between June 2009 and March 2011, the authors prospectively investigated 64 consecutive patients (33 male and 31 female) with suspected brain tumors including gliomas from prior imaging studies such as brain CT scans. All patients underwent a standard conventional MRI brain plus DTI, pMRI, and MRS. Patients with any contraindications for MRI were excluded. The present study was approved by the authors' Institutional Review Board. Written informed consents were obtained from all patients. Patients younger than 7-year-old were excluded from the study because there is a low prevalence of diffuse gliomas in this age group and to avoid any potential risk from prolonged anesthesia. All patients were provided with standard care of intracranial mass.

Reference standard

The MRI parameters were provided to the neurosurgeons prior to the surgical procedure. The patients underwent tumor resection or biopsy according to standard practice and at the discretion of the neurosurgeons. The histopathologic diagnosis and MIB-1 index were established by our experienced neuropathologist utilizing the 2007 WHO criteria. Only patients with a final pathological diagnosis of gliomas were included into the analysis.

Imaging system and sequences

All MRI sequences were performed in a single session for each patient using the same three tesla clinical MR system (Philips Achieva, Best, the Netherlands) with an 8-channel head coil utilizing the SENSE parallel imaging technique. cMRI studies included non-contrast enhancement 3D T1-weighted (T1W) with reconstruction into axial and sagittal planes, axial fluid attenuated inversion recovery (FLAIR), axial/coronal T2-weighted (T2W), and susceptibility weighted image (VenBOLD). DTI was performed before contrast administration. Post-contrast enhancement 3D-T1W sequence was achieved with reconstruction into three orthogonal planes. The dynamic susceptibility contrast (DSC) MRI was performed during the gadolinium injection, while MRS was acquired after Gd-T1W.

Diffusion tensor imaging (DTI)

DTI was acquired by using single shot spin-echo echo-planar imaging (echo/repetition time (TE/TR), 54/11,000 msec; bandwidth = 23.8 Hz; matrix, 112x112; field of view (FOV), 224 mm; EPI factor 59; slice thickness, 2.3 mm, no gap; NEX, 1; b factor = 0 and 1,000 mm^2/s; directions of gradient sampling, 16).

DSC MRI

Cerebral perfusion study was achieved during the first pass of a bolus of gadobutrol (Gadovist®; Bayer-Schering, Berlin, Germany) using a 3D Principle of Echo Shifting with a Train of Observations (PRESTO) sequence, effective TR/TE = 16/24 ms, flip angle = 7°, FOV = 230x187 mm, matrix = 64x52, slice thickness 3.5 mm, sense factor = 1.75. A series of 60 volume acquisitions was acquired at 1.2-s intervals. Ten baseline acquisitions were obtained before contrast administration. A 2 mL pre-scan contrast was intravenously injected a few minutes before the perfusion study. Then, gadobutrol (0.1 mmol/kg body weighted, maximum 7.5 mL) was injected at a rate of about 4-5 mL/sec through either an 18 or 20-gauge intravenous catheter and was followed immediately by a 10 mL saline flush. The total scan time of perfusion MRI technique was 1.16 minutes.

MR spectroscopy

The selected slices were based on Gd-T1W at the areas of lesion enhancement. If no enhanced area was demonstrated, FLAIR and T2W data was used for selecting a region of interest (ROI) by an experienced neuroradiologist judging from the pattern of signal intensity on cMRI. The solid portion of the tumor was selected for the study. Multi-voxel or single-voxel proton chemical shift MRS was used according to tumor location. For multi-voxel imaging, the turbo spin echo technique was performed with TR, TE, and NEX of 2,000, 288 msec, and 1, respectively. Single section with a 15-mm section thickness was obtained in four minutes and 42 seconds in axial plane. The volume of interest (VOI) consisted of a 10x10 cm-region placed within a 23x19 cm field of view, with a voxel size of 1x1x1.5 cm^3. Single voxel MR spectroscopy was done by using a point-resolved spectroscopy (PRESS) turbo spin echo with TR, TE of 2,000, 35/128 msec, respectively. The voxel size varied from 1x1x1 cm^3 to 2x2x2 cm^3 depending on tumor size.

Image processing and data acquisition

The findings on cMRI were independently evaluated by two neuroradiologists who were blinded from the final pathological diagnosis. Abnormal signals on T1W and T2W were visually evaluated for edema, hemorrhage, enhancement, and size of the tumors. The edema was graded (along with surrounding area of non-enhancing high SI T2W/FLAIR compared with the solid portion) into mild (less than the solid portion), moderate (equal to the solid portion), and severe (more than the solid portion) degree. Results were reached by consensus if there is any discrepancy between the two neuroradiologists.

Subsequently, post-processing analysis of MRI studies was performed on an independent workstation (Philips, Extended MR Workspace, version 2.6.3.2, Best, the Netherlands) using proprietary commercial analytic software.

For DTI (Fiber Tracking, View Forum, Philips, Best, the Netherlands), the authors measured FA and ADC values by manually placing ROIs within the enhancing region or solid non-enhancing region identified by neuroradiologists (these regions were defined as "solid tumoral region") as described in a previous report[10]. Briefly, the measured region was performed by mapping T2W, FLAIR, or post Gd-T1W with DTI data. The ROIs of 40-60 voxel were carefully placed to avoid volume averaging that might influence FA and ADC values. Each reviewer placed five ROIs in the solid tumoral region, necrotic region and the peritumoral edema regions to obtain the minimum and maximum FA and ADC values. The five ROIs were placed in normal-appearing white matter (NAWM) as well as a single ROI in genu or splenium of corpus callosum and then an average FA and ADC value was calculated. For cases with involvement of corpus callosum, the portion of corpus callosum with a normal signal on T2W was placed. The NAWM and corpus callosum were selected as the internal normal control and FA and ADC ratios of each region were established (Fig. 1, 2).

Unprocessed DSC images were analyzed on commercial software (gamma-fitted curve, ViewForum, Philips, the Netherlands). The method of measurement was as described in a separated report by the authors (in press). Briefly, the parametric color maps were evaluated and compared with co-registered 3D T1W-Gd to ensure that ROIs were not placed over blood vessels. Intra-lesional cerebral blood volume (CBV) measurements were obtained from processed CBV maps by manual ROI placement in areas of highest CBV to avoid uninvolved adjacent grey

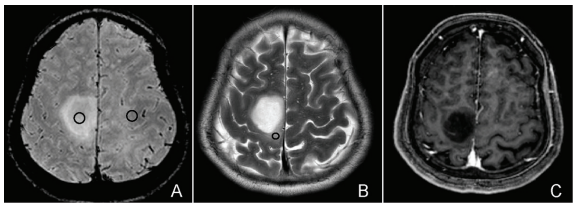

Fig. 1 Non-enhancing tumor (oligodendroglioma WHO II) at right frontal parietal region. (A) FLAIR shows ROI of solid tumoral region (right circle) and NAWM (left circle). (B) T2W shows ROI of peritumoral edema (circle). (C) Gd-T1W shows no enhancement of the mass.

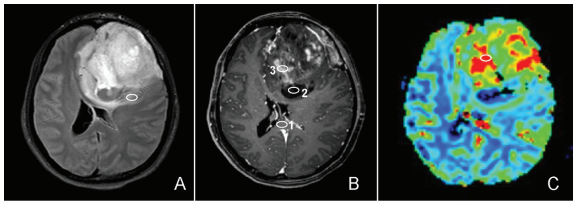

Fig. 2 Glioblastoma. (A) FLAIR shows large left frontal lobe mass with pressure effect to the lateral ventricle. The circle is ROI for peritumoral edema region. (B) Gd-T1W shows irregular enhancement of the tumor with 1 = normal posterior corpus callosum, 2 = necrotic part, and 3 = enhancing region. (C) CBV map shows ROI of enhancing region (circle).

matter structures. NAWM-ROIs were placed in the contralateral hemisphere and a maximum CBV ratio was then calculated for each tumor using the formula: rCBV = highest average CBV [lesion]/highest average CBV [contralateral white matter]. A similar measurement was performed for cerebral blood flow (i.e. CBF and rCBF) (Fig. 1, 2). The CBV and CBF measured from gamma fitted curve were relative measurements and an arbitrary unit for both parameters was obtained from the software.

The MRS data was processed on a commercial software program (Spectro-tool, ViewForum, Philips/ the Netherlands). The metabolite peaks were assigned as follows: Cho, 3.22 ppm; Cr, 3.02 ppm; NAA, 2.02 ppm; metabolite lipids, 0.5-1.5 ppm and Lactate, 1.33 ppm. The ROI was placed for measuring each metabolite at the enhanced area, peritumoral edema region, cystic/necrotic portion, and in the contralateral normal white matter. If no enhancement was seen, the solid part of the tumor was selected based on FLAIR and T2W by a neuroradiologist who was blinded from the final diagnosis. The highest values of each metabolite were collected. MRS parameters include choline (Cho), creatine (Cr), N-acetyl-aspartate (NAA), lactate (Lac), ratio of Cho/Cr, Cho/NAA, Lac/Cr, and Lac/NAA. The calculation of ratio of lesion Cho to normal Cr (nCr) and normal NAA (nNAA) was also performed for normalized Cho/nCr and Cho/nNAA, respectively.

Statistical analysis

All statistical analyses were performed using commercially available software (SPSS ver. 18, IBM, United States). The Fisher's exact test was performed in order to test the significance of differences between peritumoral edema, enhancement pattern and intratumoral hemorrhage in HGG and those in LGG on cMRI.

The mean, median, and standard deviations of the quantitative parameters from DTI, pMRI and MRS were computed in each high- and low-grade tumor. Non-parametric statistics were used for analysis of any significant difference in each variable between LGG and HGG with predetermined p-value of less than 0.05. Receiver operating characteristic (ROC) curve analysis was used to evaluate the intensity of the association between statistically significant variables and gliomas grades, as well as to determine the threshold. Sensitivity, specificity, positive predictive value (PPV), negative predictive value (NPV), and accuracy were also calculated. Logistic regression analysis was used to determine the combination of the most discriminative parameters. We also assessed diagnostic performance of the combined parameters from aMRI.

Results

Twenty of 64 cases with histopathology other than gliomas such as lymphoma, germinoma, meningioma, demyelination, cysticercosis, or metastatic cancer were excluded. The patients with cysticercosis were operated on due to having single brain lesion and clinical and imaging information appeared tumor-like. One patient with glioma withdrew from the study after surgery due to corrupted MRI data. Therefore, only 43 cases subsequently identified as having histopathologically confirmed gliomas were included in the present study. There were 25 HGGs (19 glioblastomas and 6 anaplastic astrocytomas) and 18 LGGs (16 diffuse WHO grade II gliomas [8 astrocytomas, 6 oligodendrogliomas and 2 mixed oligoastrocytomas], 1 pilocytic astrocytoma, and 1 chordoid glioma). Twenty-one cases were male and 22 were female. Patient ages ranged from 12 to 75 years (mean 45.4±14.8) (Table 1). All LGGs showed no or mild (<50% of lesion size) peritumoral edema, whereas HGGs displayed variable degrees of edema from absent to a moderate degree (50-75% of lesion size).

All HGGs demonstrated peripheral or heterogeneous enhancement, whereas half of the LGGs showed variable enhancement. Necrotic portions were identified in 15 cases (60%) of HGG and

Table 1. Demographic data of the gliomas group

Patients (n = 43)
Sex: male = 21, female = 22
Age: 12 to 75 years old (mean 45.4±14.8)
Surgical type:
Gross total resection = 11 (25.6%)
Near total resection = 12 (27.9%)
Subtotal resection = 5 (11.6%)
Partial resection = 11 (25.6%)
Cannot be assessed = 4 (9.3%)
Pathological result:
High grade gliomas (25)
Anaplastic astrocytoma = 6
Glioblastoma multiforme = 19
Low grade gliomas (18)
Diffuse WHO grade II gliomas = 16 (8 astrocytoma, 6 oligodendroglioma and 2 mixed oligoastrocytoma)
Pilocytic astrocytoma = 1
Chordoid glioma = 1

Table 2. Diagnostic performance of conventional MRI findings in differentiating HGG from LGG

Parameter	Sensitivity (%)	Specificity (%)	Accuracy (%)	PPV (%)	NPV (%)
Edema	52.0	86.7	65.0	86.7	52.0
Enhance	100.0	50.0	79.1	73.5	100.0
Hemorrhage	80.0	50.0	67.4	69.0	64.3

MRI = magnetic resonance imaging; HGG = high grade gliomas; LGG = low grade gliomas; PPV = positive predictive value; NPV = negative predictive value

in two cases (11%) of LGG. Diagnostic performance including sensitivity, specificity, accuracy, PPV, and NPV of enhancement and intratumoral hemorrhage are demonstrated in Table 2.

The result from DTI was as reported in the authors' previous study[10]. The mean FA values in the solid tumoral, necrotic and peritumoral edema regions of both LGG and HGG were lower than those of NAWM and that of the corpus callosum. The ADC and minimal ADC values of the solid tumoral region and the area of peritumoral edema, the ratio of ADC and minimal ADC of solid tumoral region relation to NAWM or corpus callosum were statistically significant to differentiate HGG from LGG ($p<0.05$). The highest predictive accuracy parameter to differentiate HGG from LGG was the ratio of minimal ADC solid tumoral region to corpus callosum (minADC/CC)(AUC = 0.7289) followed by the minimal ADC solid tumoral region (AUC = 0.711)[10].

Cerebral blood volume, flow and their ratios at the solid tumoral region were strongly associated with the glioma grades. The areas under the ROC curves for CBV, rCBV, CBF and rCBF are 0.751, 0.749, 0.762, and 0.754, respectively. The CBV at the solid tumoral region in HGG varied from 0.85 to 39.8 with a mean of 15.25±11.14 (SD), whereas that of LGG varied from 0.51 to 19.6 with a mean of 6.5±5.9 (SD).

The CBF at the solid tumoral region in HGG varied from 0.14 to 3.2 with a mean of 1.35±0.82, whereas that of LGG varied from 0.06 to 2.66 with a mean of 0.7±0.7. On the basis of equal misclassification rates, a cut-off value of 2.4 for the rCBV (sensitivity, 88.9%; specificity, 64.7%), and a cut-off value of 2.6 for the rCBF (sensitivity, 85.2%; specificity, 70.6%) optimally discriminated HGG from LGG (Table 3).

Of 43 patients, 40 had appropriate quality of MRS spectra for interpretation. The MRS analysis showed significant difference of NAA, Cr, and Cho/Cr between HGG and LGG at the solid tumoral region. The median (minimum-maximum) values of each group are demonstrated in Table 4. The threshold of Cho/Cr ratios for identifying HGG were chosen at 1.7, 2, and 2.7 for analysis of diagnostic performance. The best discriminating ratio was 1.7 with high sensitivity for HGG.

Table 3. Results of pMRI measurement comparing between HGG and LGG

Parameter (mean ± SD)	Low-grade	High-grade	p-value
CBV			
Solid tumoral region	6.5±5.9	15.2±11.1	0.004
Peritumoral edema	1.8±1.3	1.6±0.86	0.566
Contralateral NAB	1.9±1.1	1.9±0.75	0.662
CBF			
Solid tumoral region	0.7±0.7	1.3±0.8	0.010
Peritumoral edema	0.2±0.15	0.2±0.13	0.923
Contralateral NAB	0.2±0.11	0.2±0.09	0.690
CBV ratio			
Solid tumor/NAB	3.9±4.1	8.3±5.8	0.009
CBF ratio			
Solid tumor/NAB	3.2±3.5	5.7±3.7	0.032

pMRI = perfusion magnetic resonance imaging; CBV = cerebral blood volume; CBF = cerebral blood flow; NAB = contralateral normal appearing brain parenchyma

Analysis of combined parameters from aMRI

The authors chose the threshold of the parametric measurement in each modality, which provided the best accuracy and acceptable sensitivity and specificity for differentiating HGG from LGG. The ratio equal to or higher than 2.4 for rCBV, 2.6 for rCBF, 1.7 for Cho/Cr, and ratio equal to or lower than 1.6 for minADC/CC at the solid tumoral region were chosen. The logistic regression analysis and diagnostic performance of each parameter as well as variable combination of the parameters are shown in Table 5. The results show that the combination of rCBV, Cho/Cr and minADC/CC offered the best sensitivity and NPV and the combination of rCBV and Cho/Cr displayed the best specificity and positive predictive value. The probability of having a HGG was 0.889 if all parameters were equal or higher than the determined threshold.

Table 4. Results of MRS measurement comparing between HGG and LGG

Parameter	Low-grade median (min-max)	High-grade median (min-max)	p-value
Solid tumoral region			
NAA	181.3 (21.2-444.0)	72.0 (32.2-676.1)	0.049
Choline	278.5 (171.3-4247.1)	264.2 (67.5-991.4)	0.201
Creatine	154.4 (42.7-1261.8)	86.9 (19.8-626.6)	0.008
Lipid/lactate	0.4 (0.3-5.9)	0.9 (0.04-21.87)	0.138
Solid tumoral region			
Cho/NAA	2.6 (0.7-27.5)	2.7 (0.7-9.2)	0.659
Cho/Cr	1.9 (1.3-10.5)	2.5 (1.5-5.5)	0.032
Cho/nNAA	0.7 (0.4-12.5)	0.7 (0.2-5.9)	0.162
Cho/nCr	1.8 (0.8-64.9)	2.0 (0.7-24.1)	0.443

MRS = magnetic resonance spectroscopy; NAA = N-acetyl-aspartate; Cho = choline; Cr = creatine; nNAA = NAA of contralateral normal brain; nCr = creatine of contralateral normal brain

Table 5. Diagnostic performance of parametric measurements from advanced MRI study in differentiating HGG from LGG

Parameters	Sensitivity (%)	Specificity (%)	Accuracy (%)	PPV (%)	NPV (%)
rCBV (2.4)	88.0	61.1	76.7	75.9	78.6
rCBF (2.6)	84.0	66.7	76.7	77.8	75.0
Cho/Cr (1.7)	91.7	37.5	70.0	68.6	75.0
minADC/CC (1.6)	84.0	55.6	72.1	72.4	71.4
Combination					
rCBV + minADC/CC	88.0	61.1	76.7	75.9	78.6
rCBV + Cho/Cr	79.2	75.0	77.5	82.6	70.6
rCBV + minADC/CC + Cho/Cr	87.5	68.8	80.0	80.8	78.6

rCBV = cerebral blood volume ratio; rCBF= cerebral blood flow ratio; minADC/CC = minimum apparent diffusion coefficient of solid tumor to corpus callosum

Discussion

Maximum safe resection has been accepted as the first line treatment for both LGG and HGG as it seems to confer a survival benefit from several retrospective studies[11]. However, post-operative treatment varies considerably according to histologic grade. Pathological diagnosis with accurate grading requires not only adequate but also proper tissue sampling[12]. The present study attempted to demonstrate that comprehensive study with cMRI and aMRI provides more accurate pre-operative glioma grading than cMRI alone. Many previous studies revealed that aMRI could predict glioma grading by comparing aMRI parameters to focal tissue from stereotactic biopsy[13]. However, in routine clinical practice, radiologists interpret the findings from the whole lesion. The authors therefore designed the present study to simulate actual clinical practice and to evaluate the diagnostic performance of aMRI for glioma grading. Most parametric measurements from aMRI displayed low specificity to differentiate HGG from LGG in the present study. The highest specificity derived from the combination of MRS and pMRI. Although the addition of DTI data to MRS and pMRI was associated with slightly lower specificity, the higher sensitivity and NPV made this combination more intriguing. In practice, clinicians need both high sensitivity in order not to miss HGG and high specificity to avoid unnecessary aggressive treatment for LGG. The combination of all aMRI parameters offer useful information about glioma grading required for proper patient management. The important pitfall of aMRI was associated with technical problems. Motion effect and field inhomogeneity affected data quality of the modalities utilized. In the present study, the parameters most affected by these variables were MRS followed by DTI. Perfusion MRI seemed to be the most robust modality due to rapid scan time. However, susceptibility to artifacts and the pMRI algorithm used in the present study resulted in unsatisfactory diagnostic performance when compared to other previous reports[9,14]. The inherent technical challenge is still

difficult to overcome even with the ongoing technological advances in MR machine hardware and associated software. This causes a degree of apprehension among radiologists, who perform imaging studies for patients with brain tumors. Launching this project has changed the perception of our radiologists. With the constrained scan time and very tight schedule of our MR machine (only one for a 2,500-bed medical center), the authors also needed to familiarize our department personnel with aMRI procedures as much as possible. At the end of the study, the authors' Department of Radiology adopted the aMRI protocol as a routine clinical procedure for patients with suspected gliomas. The results from the present study were in line with the study by Zonari et al[15]. The authors concur rCBV to be the most important parameter in discriminating HGG from LGG. The authors also found the high sensitivity of Cho/Cr with low specificity. Addition of Cho/Cr ratio to the other two combinations did not affect the sensitivity but improved the specificity. On the other hand, minADC/CC improved the sensitivity but compromised the specificity. In practice, the most repeatable measurement with high confidence and low variation among radiologists and technicians are CBV and MRS. Measurement of ADC is not commonly done. Most radiologists interpret DTI by visual assessment of signal intensity (SI) on DWI/ADC maps. A ratio of 1.6 of minADC/CC, illustrates that there are still some cases of HGG with higher SI than the corpus callosum. Certain cases of HGG cannot be separated from LGG by visual assessment. From this point of view, the authors proposed using quantitative parameters by combining rCBV and Cho/Cr to differentiate between HGG and LGG. The results from this study may have clinical implications. For instance, if the patient's aMRI is consistent with HGG but the stereotactic brain biopsy reveals LGG, a close clinical follow-up or empiric treatment protocols for HGG may be considered. In addition, aMRI may be helpful to rule out malignant transformation of LGG during the longitudinal imaging surveillance for an individual patient.

The results of both aMRI and cMRI were provided to the surgeons and might cause bias for decision in surgical procedure. This limitation could not be avoided due to ethical issue but certainly affected the pathological results of the un-resected part of the tumors. However, in our hospital, usually the surgeons resected all benign and malignant tumors as much as possible relying on anatomical images and surgical

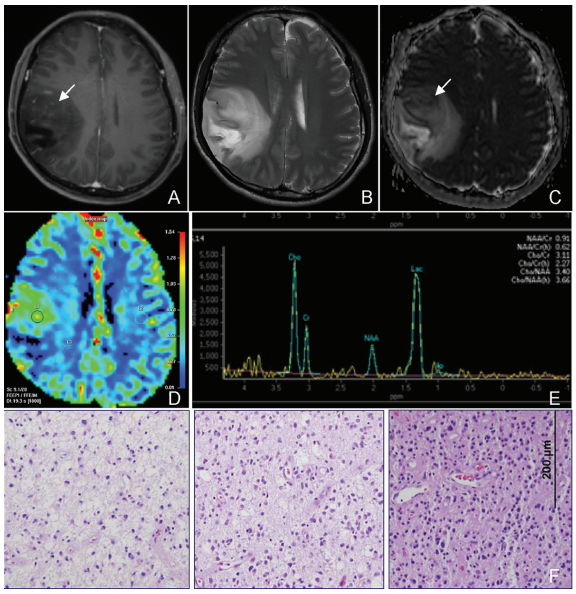

Fig. 3 Thirty-six years old male presented with seizure and left sided numbness. The cMRI (A) Gd-T1W, (B) T2W demonstrated a mass at right frontoparietal region with suspected tiny spots of enhancement at the anterior part (arrow in A), (C) ADC map showed corresponding area of less ADC than other part of the tumor, (D) CBV map showed high perfusion of the mass, (E) MRS showed increased Cho and Lac peaks, (F) Three areas with different pathological grade of the tumor were found. The final diagnosis was anaplastic astrocytoma, WHO III (MIB-1 index 10-12%).

findings as well as the judgment of patient outcome. One example of a case that aMRI provided clinical relevant was shown in Fig. 3. This 36-year-old male was diagnosed by aMRI as having a high-grade tumor due to high rCBV and Cho/Cr. Intraoperatively, the frozen section was reported as diffuse astrocytoma, WHO grade II. The surgeon still performed total resection. The pathologist was concerned with the radiological report and found three areas with different grades of tumor from the surgical specimen. The patient was finally diagnosed as anaplastic astrocytoma, WHO grade III (MIB-1 index = 10-12%).

In conclusion, incorporation of aMRI into routine evaluation of gliomas is feasible even in a resource-limited setting and it provides better accuracy than cMRI in differentiating HGG from LGG. Combination of rCBV and Cho/Cr at the predetermined threshold was the most practical modality with an acceptable sensitivity and specificity.

Acknowledgement

The present study was funded by the Faculty of Medicine Siriraj Hospital, Mahidol University. The authors wish to thank the following persons, who provided helpful suggestions for the present study: Nanthasak Tisavipat, Akkapong Nitising, Sarun Nuntaaree, Prajak Srirabhebhat, Vutisiri Veerasarn, Nanta Kietkanwankei, Sureerat Thummalungka, Prapaporn Pornpunyawuth, Anchalee Chorojana, Pipat Chiewwit, Chulaluk Komoltri, and Surachai Likasitwattankul. The authors also would like to thank Thomas for reviewing the manuscript.

What is already known from this topic?

1. Many previous studies revealed that aMRI could predict glioma grading by comparing aMRI parameters to focal tissue from stereotactic biopsy[13].

2. The important pitfall of aMRI was associated technical problems. Motion effect and field inhomogeneity affected data quality of the modalities utilized. Perfusion MRI seemed to be the most robust modality due to rapid scan time. However, susceptibility to artifacts and the pMRI algorithm used in this study resulted in unsatisfactory diagnostic performance when compared to other previous reports[9,14]. The inherent technical challenge is still difficult to overcome even with the ongoing technological advances in MR machine hardware and associated software. This causes a degree of apprehension among radiologists, who perform imaging studies for patients with brain tumors.

What this study adds?

1. Most parametric measurements from aMRI displayed low specificity to differentiate HGG from LGG in this study. The highest specificity derived from the combination of MRS and pMRI.

The combination of all aMRI parameters offer useful information about glioma grading required for proper patient management.

2. The authors proposed using quantitative parameters by combining rCBV and Cho/Cr to differentiate between HGG and LGG.

3. Launching this project has changed the perception of our radiologists. With the constrained scan time and very tight schedule of our MR machine, we also needed to familiarize our department personnel with aMRI procedures as much as possible.

4. Most radiologists interpret DTI by visual assessment of signal intensity (SI) on DWI/ADC maps. A ratio of 1.6 of minADC/CC, illustrates that there are still some cases of HGG with higher SI than the corpus callosum. Certain cases of HGG cannot be separated from LGG by visual assessment.

Abbreviations

LGG = low grade gliomas; HGG = high grade gliomas; MRI = magnetic resonance imaging; cMRI = conventional MRI; aMRI = advanced MRI; pMRI = perfusion MRI, DTI = diffusion tensor imaging; MRS = magnetic resonance spectroscopy; DSC = dynamic susceptibility contrast; T1W = T1-weighted image; T2W = T2 weighted imaging; FLAIR, fluid attenuated inversion recovery; SWI = susceptibility weighted image; Gd = gadolinium; PRESTO = Principle of Echo Shifting with a Train of Observations; PRESS = point-resolved spectroscopy; ROI = region of interest; CBV = cerebral blood volume; CBF = cerebral blood flow; ADC = apparent diffusion coefficient; FA = fractional anisotropy; minADC = the minimum ADC value; CC = corpus callosum; NAWM = normal appearing white matter; Cho = choline; Cr = creatine; NAA = N-acetyl-aspartate; Lac = lactate; PPV = positive predictive value; NPV = negative predictive value

Potential conflicts of interest

None.

References

1. Wen PY, Kesari S. Malignant gliomas in adults. N Engl J Med 2008; 359: 492-507.
2. Jacobs AH, Kracht LW, Gossmann A, Ruger MA, Thomas AV, Thiel A, et al. Imaging in neurooncology. NeuroRx 2005; 2: 333-47.
3. Guo AC, Cummings TJ, Dash RC, Provenzale JM. Lymphomas and high-grade astrocytomas: comparison of water diffusibility and histologic characteristics. Radiology 2002; 224: 177-83.
4. Christoforidis GA, Yang M, Kontzialis MS, Larson DG, Abduljalil A, Basso M, et al. High resolution ultra high field magnetic resonance imaging of glioma microvascularity and hypoxia using ultra-small particles of iron oxide. Invest Radiol 2009; 44: 375-83.
5. Folkman J. Angiogenesis in cancer, vascular, rheumatoid and other disease. Nat Med 1995; 1: 27-31.
6. Kondziolka D, Lunsford LD, Martinez AJ. Unreliability of contemporary neurodiagnostic imaging in evaluating suspected adult supratentorial (low-grade) astrocytoma. J Neurosurg 1993; 79: 533-6.
7. Knopp EA, Cha S, Johnson G, Mazumdar A,

Golfinos JG, Zagzag D, et al. Glial neoplasms: dynamic contrast-enhanced T2*-weighted MR imaging. Radiology 1999; 211: 791-8.
8. Essig M, Anzalone N, Combs SE, Dorfler A, Lee SK, Picozzi P, et al. MR imaging of neoplastic central nervous system lesions: review and recommendations for current practice. AJNR Am J Neuroradiol 2012; 33: 803-17.
9. Law M, Yang S, Wang H, Babb JS, Johnson G, Cha S, et al. Glioma grading: sensitivity, specificity, and predictive values of perfusion MR imaging and proton MR spectroscopic imaging compared with conventional MR imaging. AJNR Am J Neuroradiol 2003; 24: 1989-98.
10. Piyapittayanan S, Chawalparit O, Tritakarn SO, Witthiwej T, Sangruchi T, Nunta-Aree S, et al. Value of diffusion tensor imaging in differentiating high-grade from low-grade gliomas. J Med Assoc Thai 2013; 96: 716-21.
11. Stupp R, Mason WP, van den Bent MJ, Weller M, Fisher B, Taphoorn MJ, et al. Radiotherapy plus concomitant and adjuvant temozolomide for glioblastoma. N Engl J Med 2005; 352: 987-96.
12. Watanabe M, Tanaka R, Takeda N. Magnetic resonance imaging and histopathology of cerebral gliomas. Neuroradiology 1992; 34: 463-9.
13. Weber MA, Henze M, Tuttenberg J, Stieltjes B, Meissner M, Zimmer F, et al. Biopsy targeting gliomas: do functional imaging techniques identify similar target areas? Invest Radiol 2010; 45: 755-68.
14. Shin JH, Lee HK, Kwun BD, Kim JS, Kang W, Choi CG, et al. Using relative cerebral blood flow and volume to evaluate the histopathologic grade of cerebral gliomas: preliminary results. AJR Am J Roentgenol 2002; 179: 783-9.
15. Zonari P, Baraldi P, Crisi G. Multimodal MRI in the characterization of glial neoplasms: the combined role of single-voxel MR spectroscopy, diffusion imaging and echo-planar perfusion imaging. Neuroradiology 2007; 49: 795-803.

คุณภาพในการวินิจฉัยแยกโรคเนื้องอกสมองไกลโอมาชนิดร้ายแรงจากไม่ร้ายแรงด้วยเอ็มอาร์ไอก้าวหน้าในเวชปฏิบัติ

อรสา ชวาลภาฤทธิ์, ตุ้มทิพย์ แสงรุจิ, ธีรพล วิทธิเวช, สิทธิ์ สาธรสุเมธี, สิริอร ตริตระการ, ศิริวรรณ ปิยะพิทยนันท์, ประภาลักษณ์ ชัยเจริญ, ธันยพร ดิเรกสุนทร, พนิดา ชาญเชาว์วานิช

วัตถุประสงค์: *เพื่อประเมินคุณภาพของการใช้เอ็มอาร์ไอก้าวหน้าในการแยกเนื้องอกสมองไกลโอมาชนิดร้ายแรงออกจากไม่ร้ายแรง*
วัสดุและวิธีการ: *ผู้ป่วย 64 ราย ที่ได้รับการวินิจฉัยเบื้องต้นว่าอาจเป็นเนื้องอกสมองชนิดไกลโอมา ได้รับการตรวจเอ็มอาร์ไอปกติและก้าวหน้า ซึ่งรวมถึง MR spectroscopy, diffusion MRI, และ dynamic susceptibility perfusion MRI ภาพเอ็มอาร์ไอที่ได้ถูกนำมาแปลผล และวัดหรือคำนวณหาค่า fractional anisotropy, apparent diffusion coefficient (ADC), cerebral blood flow และ volume, และสัดส่วนของ choline ต่อ creatine ของเนื้องอกเปรียบเทียบกับเนื้อสมองปกติ*
ผลการศึกษา: *มีผู้ป่วยที่ได้รับการวินิจฉัยทางพยาธิวิทยาว่าเป็นเนื้องอกสมองไกลโอมา 43 ราย ตัวแปรที่ใช้แยกชนิดร้ายแรงออกจากไม่ร้ายแรงที่ดีที่สุดคือ cerebral blood flow และ volume ของเนื้องอก ในขณะที่สัดส่วนของค่าต่ำสุดของ ADC ของเนื้องอกต่อ corpus callosum และสัดส่วนของ choline ต่อ creatine ของเนื้องอกจะให้คุณภาพในการแยกโรคได้ดีที่สุดเมื่อกำหนดค่าตัดของตัวแปรที่วัดในการแยกชนิดร้ายแรงจากไม่ร้ายแรง การใช้ตัวแปรหลายตัวร่วมกันจะให้ความแม่นยำสูงสุด ขณะที่การใช้ค่าตัดจาก MR spectroscopy และ dynamic susceptibility perfusion MRI จะให้ความจำเพาะสูงสุด และเมื่อตัวแปรทุกตัวมีผลเป็นบวก ความเป็นไปได้ที่เนื้องอกชนิดนั้นจะเป็นชนิดร้ายแรงเท่ากับ 0.889*
สรุป: *ในการแยกเนื้องอกไกลโอมาชนิดร้ายแรง เอ็มอาร์ไอก้าวหน้าจะมีคุณภาพในการวินิจฉัยแยกโรคได้ดีกว่าการประเมินลักษณะของเนื้องอกจากภาพเอ็มอาร์ไอธรรมดาอย่างเดียว*